The Annals of Applied Statistics
2015, Vol. 9, No. 1, 122–144
DOI: 10.1214/14-AOAS789

REACTIVE POINT PROCESSES: A NEW APPROACH TO PREDICTING POWER FAILURES IN UNDERGROUND ELECTRICAL SYSTEMS[1]

BY ŞEYDA ERTEKIN*, CYNTHIA RUDIN* AND TYLER H. MCCORMICK†

*Massachusetts Institute of Technology** *and University of Washington*†

Reactive point processes (RPPs) are a new statistical model designed for predicting discrete events in time based on past history. RPPs were developed to handle an important problem within the domain of electrical grid reliability: short-term prediction of electrical grid failures ("manhole events"), including outages, fires, explosions and smoking manholes, which can cause threats to public safety and reliability of electrical service in cities. RPPs incorporate self-exciting, self-regulating and saturating components. The self-excitement occurs as a result of a past event, which causes a temporary rise in vulner ability to future events. The self-regulation occurs as a result of an external inspection which temporarily lowers vulnerability to future events. RPPs can saturate when too many events or inspections occur close together, which ensures that the probability of an event stays within a realistic range. Two of the operational challenges for power companies are (i) making continuous-time failure predictions, and (ii) cost/benefit analysis for decision making and proactive maintenance. RPPs are naturally suited for handling both of these challenges. We use the model to predict power-grid failures in Manhattan over a short-term horizon, and to provide a cost/benefit analysis of different proactive maintenance programs.

1. Introduction. We present a new statistical model for predicting discrete events over time, called Reactive Point Processes (RPPs). RPPs are a natural fit for many different domains, and their development was motivated by the problem of predicting serious events (fires, explosions, power failures) in the underground electrical grid of New York City (NYC). In New York City and in other major urban centers, power-grid reliability is a major source of concern, as demand for electrical power is expected to soon exceed the amount we are able to deliver with our current infrastructure [DOE (2008), NYBC (2010), Rhodes (2013)]. Many American electrical grids are massive and have been built gradually since the time of Thomas Edison in the 1880s. For instance, in Manhattan alone, there are over 21,216 miles of underground cable, which is almost enough cable to wrap once around the earth. Manhattan's power distribution system is the oldest in the world,

Received July 2014; revised September 2014.

[1]Supported in part by Con Edison, the MIT Energy Initiative Seed Fund and NSF CAREER Grant IIS-1053407 to C. Rudin.

Key words and phrases. Point processes, self-exciting processes, energy grid reliability, Bayesian analysis, time-series.

and NYC's power utility company, Con Edison, has cable databases that started in the 1880s. Within the last decade, in order to handle increasing demands on NYC's power-grid and increasing threats to public safety, Con Edison has developed and deployed various proactive programs and policies [So (2004)]. In Manhattan, there are approximately 53,000 access points to the underground electrical grid, which are called electrical service structures or manholes. Problems in the underground distribution network are manifested as problems within manholes, such as underground burnouts or serious events. A multi-year, ongoing collaboration to predict these events in advance was started in 2007 [Rudin et al. (2010, 2012, 2014)], where diverse historical data were used to predict manhole events over a long-term horizon, as the data were not originally processed enough to predict events in the short term. Being able to predict manhole events accurately in the short term could immediately lead to reduced risks to public safety and increased reliability of electrical service. The data from this collaboration have sufficiently matured due to iterations of the knowledge discovery process and maturation of the Con Edison inspections program, and, in this paper, we show that it is indeed possible to predict manhole events to some extent within the short term.

The fact that RPPs are a generative model allows them to be used for cost-benefit analysis, and thus for policy decisions. In particular, since we can use RPPs to simulate power failures into the future, we can also simulate various inspection policies that the power company might implement. This way we can create a robust simulation setup for evaluating the relative costs of different inspection policies for NYC. This type of cost-benefit analysis can quantify the cost of the inspections program as it relates to the forecasted number of manhole events.

RPPs capture several important properties of power failures on the grid:

- There is an instantaneous rise in vulnerability to future serious events immediately following an occurrence of a past serious event, and the vulnerability gradually fades back to the baseline level. This is a type of *self-exciting* property.
- There is an instantaneous decrease in vulnerability due to an inspection, repair or other action taken. The effect of this inspection fades gradually over time. This is a *self-regulating* property.
- The cumulative effect of events or inspections can saturate, ensuring that vulnerability levels never stray too far beyond their baseline level. This captures *diminishing returns* of many events or inspections in a row.
- The baseline level can be altered if there is at least one past event.
- Vulnerability between similar entities should be similar. RPPs can be incorporated into a Bayesian framework that shares information across observably similar entities.

RPPs extend self-exciting point processes (SEPPs), which have only the self-exciting property mentioned above. Self-exciting processes date back at least to the 1960s [Bartlett (1963), Kerstan (1964)]. The applicability of self-exciting

point processes for modeling and analyzing time-series data has stimulated interest in diverse disciplines, including seismology [Ogata (1988, 1998)], criminology [Egesdal et al. (2010), Lewis et al. (2010), Louie, Masaki and Allenby (2010), Mohler et al. (2011), Porter and White (2012)], finance [Aït-Sahalia, Cacho-Diaz and Laeven (2010), Bacry et al. (2013), Chehrazi and Weber (2011), Embrechts, Liniger and Lin (2011), Filimonov and Sornette (2012), Hardiman, Bercot and Bouchaud (2013)], computational neuroscience [Johnson (1996), Krumin, Reutsky and Shoham (2010)], genome sequencing [Reynaud-Bouret and Schbath (2010)] and social networks [Crane and Sornette (2008), Du et al. (2013), Masuda et al. (2012), Mitchell and Cates (2010), Simma and Jordan (2010)]. These models appear in so many different domains because they are a natural fit for time-series data where one would like to predict discrete events in time, and where the occurrence of a past event gives a temporary boost to the probability of an event in the future. A recent work on Bayesian modeling for dependent point processes is that of Guttorp and Thorarinsdottir (2012). Paralleling the development of frequentist literature, many Bayesian approaches are motivated by data on natural events. Peruggia and Santner (1996), for example, develop a Bayesian framework for the Epidemic-Type-Aftershock-Sequences (ETAS) model. Nonparametric Bayesian approaches for modeling data from nonhomogeneous point pattern data have also been developed [see Taddy and Kottas (2012), e.g.]. Blundell, Beck and Heller (2012) present a nonparametric Bayesian approach that uses Hawkes models for relational data. An expanded related work section appears in the supplementary material [Ertekin, Rudin and McCormick (2015)].

The self-regulating property can be thought of as the effect of an inspection. Inspections are made according to a predetermined policy of an external source, which may be deterministic or random. In the application that self-exciting point processes are the most well known for, namely, earthquake modeling, it is not possible to take an action to preemptively reduce the risk of an earthquake; however, in other applications it is clearly possible to do so. In our power failure application, power companies can perform preemptive inspections and repairs in order to decrease electrical grid vulnerability. In neuroscience, it is possible to take an action to temporarily reduce the firing rate of a neuron. There are many actions that police can take to temporarily reduce crime in an area (e.g., temporary increased patrolling or monitoring). In medical applications, doses of medicine can be preemptively applied to reduce the probability of a cardiac arrest or other event. Alternatively, for instance, the self-regulation can come as a result of the patient's lab tests or visits to a physician.

Another way that RPPs expand upon SEPPs is that they allow deviations from the baseline vulnerability level to saturate. Even if there are repeated events or inspections in a short period of time, the vulnerability level still stays within a realistic range. In the original self-exciting point process model, it is possible for the self-excitation to escalate to the point where the probability of an event gets very close to one, which is generally unrealistic. In RPPs, the saturation function

prevents this from happening. Also, if many inspections are done in a row, the vulnerability level does not drop to zero, and there are diminishing returns for the later ones because of the saturation function.

Outline of paper. We motivate RPPs using the power-grid application in Section 2. We first introduce the general form of the RPP model in Section 3. We discuss a Bayesian framework for fitting RPPs in Section 4. The Bayesian formulation, which we implement using Approximate Bayesian Computation (ABC), allows us to share information across observably similar entities (manholes in our case). For both methods we fit the model to NYC data and performed simulation studies. Section 5 contains a prediction experiment, demonstrating the RPPs' ability to predict future events in NYC. Once the RPP model is fit to data from the past, it can be used for simulation. In particular, we can simulate various inspection policies for the Manhattan grid and examine the costs associated with each of them in order to choose the best inspection policy. Section 6 shows this type of simulation using the RPP, illustrating how it is able to help choose between different inspection policies, and thus assist with broader policy decisions for the NYC inspections program. The paper's supplementary material [Ertekin, Rudin and McCormick (2015)] includes a related work section, conditional frequency estimator (CF estimator) for the RPP, experiments with a maximum likelihood approach, a description of the inspection policy used in Section 6 and simulation studies for validating the fitting techniques for the models in the paper. It also includes a description and link for a publicly available simulated data set that we generated, based on statistical properties of the Manhattan data set.

A short version of this paper appeared in the late-breaking developments track of AAAI-13 [Ertekin, Rudin and McCormick (2013)].

2. Description of data. The data used for the project includes records from the Emergency Control Systems (ECS) trouble ticket system of Con Edison, which includes records of responses to past events (total 213,504 records for 53,525 manholes from 1995 until 2010). Part of the trouble ticket for a manhole fire is in Figure 1.

Events can include serious problems such as manhole fires or explosions, or nonserious events such as wire burnouts. These tickets are heavily processed into a structured table, where each record indicates the time, manhole type ("service box" or "manhole," and we refer to both types as manholes colloquially), the unique identifier of the manhole and details about the event. The trouble tickets are classified automatically as to whether they represent events (the kind we would like to predict and prevent) or not (in which case the ticket is irrelevant and removed). The processing of tickets is based on a study where Con Edison engineers manually labeled tickets, and is discussed further by Passonneau et al. (2011).

```
FDNY/250 REPORTS F/O 45536 E.51 ST & BEEKMAN PL...MANHOLE FIRE
MALDONADO REPORTS F/O 45536 E.51 ST FOUND SB-9960012 SMOKING
HEAVY...ACTIVE...SOLID...ROUND...NO STRAY VOLTAGE...29-L...
SNOW...FLUSH REQUESTED...ORDERED #100103.
12/22/09 08:10 MALDONADO REPORTS 3 2WAY-2WAY CRABS COPPERED
CUT OUT & REPLACED SAME. ALSO STATES 5 WIRE CROSSING COMES U
P DEAD WILL INVESTIGATE IN SB-9960013.
FLUSH # 100116 ORDERED FOR SAME
12/22/09 14:00 REMARKS BELOW WERE ADDED BY 62355
12/22/09 01:45 MASON REPORTS F/O 4553 E.51ST CLEARED ALL
B/O-S IN SB9960013 ALSO FOUND A MAIN MISSING FROM THE WEST IN
12/22/09 14:08 REMARKS BELOW WERE ADDED BY 62355
SB9960011 F/O 1440 BEEKMAN.............................JMC
```

FIG. 1. *Part of the ECS remarks from a manhole fire ticket in* 2009. *The ticket implies that the manhole was actively smoking upon the worker's arrival. The worker located a crab connector that had melted* (*"coppered"*) *and a cable that was not carrying current* (*"dead"*). *Addresses and manhole numbers were changed for the purpose of anonymity.*

We have more or less complete event data from 1999 until the present, and incomplete event data between 1995 and 1999. A plot of the total number of events per year (using our definition of what constitutes an event) is provided in Figure 2(a).

We also have manhole location and cable record information, which contains information about the underground electrical infrastructure. These two large tables are joined together to determine which cables enter into which manholes. The inferential join between the two tables required substantial processing in order to correctly match cables with manholes. *Main cables* are cables that connect two manholes, as opposed to *service* or *streetlight cables* which connect to buildings or streetlights. In our studies on long-term prediction of power failures, we have found that the number of main phase cables in a manhole is a relatively useful indicator of whether a manhole is likely to have an event. Figure 2(b) contains a histogram of the number of main phase cables in a manhole.

The electrical grid was built gradually over the last $\sim$130 years, and, as a result, manholes often contain cables with a range of different ages. Figure 2(c) contains a histogram of the age of the oldest main cables in each manhole, as recorded in the database. Cable age is also used as a feature for our RPP model. Cable ages range from less than a year old to over 100 years old; Con Edison started keeping records back in the 1880s during the time of Thomas Edison. We remark that it is not necessarily true that the oldest cables are the ones most in need of replacement. Many cables have been functioning for a century and are still functioning reliably.

We also have data from Con Edison's new inspections program. Inspections can be scheduled in advance, according to a schedule determined by a state mandate. This mandate currently requires an inspection for each structure at least once every 5 years. Con Edison also performs "ad hoc" inspections. These occur when

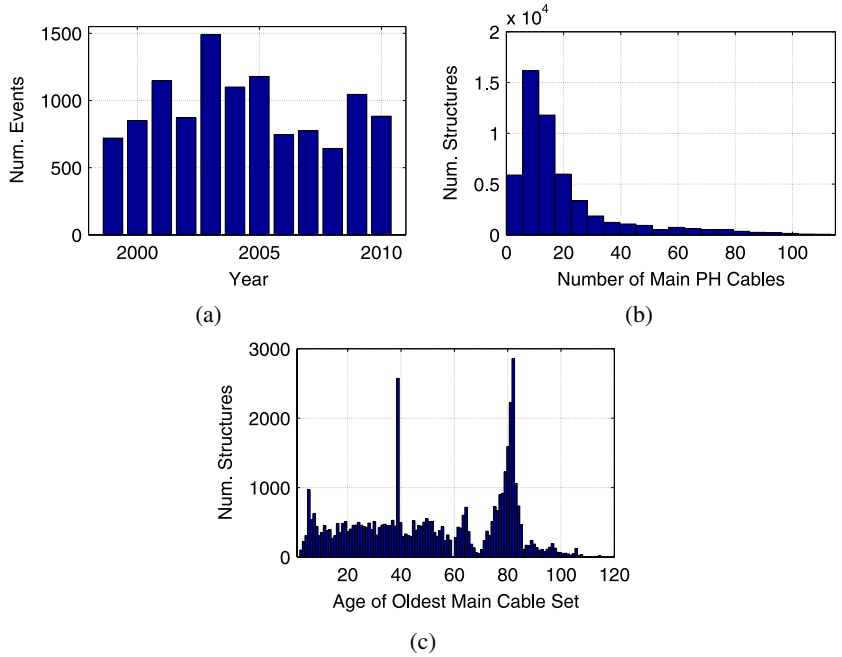

FIG. 2. *A plot of the number of yearly events, a histogram of the number of Main Phase (PH) cables, and a histogram of the age of oldest cable set in a manhole.*

a worker is inside a manhole for another purpose (e.g., to connect a new service cable) and chooses to fill in an inspection form. The inspections are broken down into 5 distinct types, depending on whether repairs are urgent (Level I) or whether the inspector suggests major infrastructure repairs (Level IV) that are placed on a waiting list to be completed. Sometimes when continued work is being performed on a single manhole, this manhole will have many inspections performed within a relatively small amount of time—hence our need for "diminishing returns" on the influence of an inspection that motivates the saturation function of the RPP model.

Some questions of interest to power companies are as follows:

(i) Can we predict failures continuously in time, and can we model how quickly the influence of past events and inspections fade over time?

(ii) Can we develop a cost/benefit analysis for proactive maintenance policies?

RPPs will help with both of these questions.

3. The reactive point process model. We begin with a simpler version of RPPs where there is only one time-series corresponding to a single entity (manhole). Our data consist of a series of N_E events with event times $t_1, t_2, \ldots, t_{N_E}$ and a series of given inspection times denoted by $\bar{t}_1, \bar{t}_2, \ldots, \bar{t}_{N_I}$. The inspection times are assumed to be under the control of the experimenter. RPPs model events

as being generated from a nonhomogeneous Poisson process with intensity $\lambda(t)$ where

$$\lambda(t) = \lambda_0\Bigg[1 + g_1\Bigg(\sum_{\forall t_e < t} g_2(t - t_e)\Bigg) - g_3\Bigg(\sum_{\forall \bar{t}_i < t} g_4(t - \bar{t}_i)\Bigg) + C_1 \mathbf{1}_{[N_E \geq 1]}\Bigg], \tag{1}$$

where t_e are event times and $\bar{t}_i$ are inspection times. The vulnerability level permanently goes up by C_1 if there is at least one past event, where C_1 is a constant that can be fitted. The $C_1\mathbf{1}_{[N_E \geq 1]}$ term is present to deal with "zero inflation," where the case of zero events needs to be handled separately than one or more past events. Functions g_2 and g_4 are the self-excitation and self-regulation functions, which have initially large amplitudes and decay over time. Self-exciting point processes have only g_2, and not the other functions, which are novel to RPPs. Functions g_1 and g_3 are the saturation functions, which start out as the identity function and then flatten farther from the origin. If the total sum of the excitation terms is large, g_1 will prevent the vulnerability level from increasing too much. Similarly, g_4 controls the total possible amount of self-regulation and encodes "diminishing returns" for having several inspections in a row.

The RPP model arose based on exploratory work performed using a conditional frequency (CF) estimator of the data. To construct the CF estimator, we computed the empirical probability of another event occurring on a day t given that an event occurred at $t = 0$. To obtain these probabilities, we first align the sequences of time so that $t = 0$ represents the time when an event happened. We now have a series of "trails" that give the probability of another event, conditional on the last event that occurred for a given manhole. We used only trails that were far apart in time so we could look at the effect of each event without considering short-term influences of other previous events. What we see from Figure 3(a) is that the conditional probability for experiencing a second event soon after the first event is high and decays with t. This decay represents self-exciting behavior. To see evidence of self-excitation from the raw data, we present plots of event times for several manholes in Figure 4. We see a clear grouping of events which is consistent with self-exciting behavior. These observations lead us to include the g_2 term in (1). The behavior we observe could not be easily explained using a simple random effects model; an attempt to do this is within Section 4 of the supplementary material [Ertekin, Rudin and McCormick (2015)].

Next, we evaluate whether subsequent events continue to increase propensity for another event or whether the risk in the most troubled manholes "saturates" and multiple manhole events in a row have diminishing-returns on the conditional probabilities. Figure 3(b) shows the saturation effect. The y-axis of this plot contains raw empirical probabilities of another event. The x-axis are sums of effects from previous recent events (sums of g_2 values). If Figure 3(b) were linear, we would not see diminishing returns. That is, a linear trend in Figure 3(b) would indicate that each subsequent event increases the likelihood of another event by

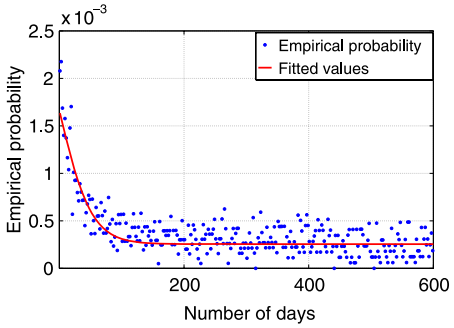

(a) Empirical probabilities and fitted values for the self-excitation function g_2

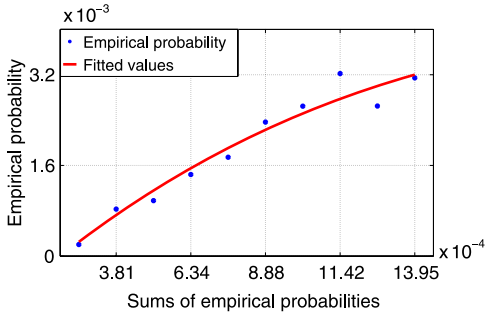

(b) Empirical probabilities and fitted values for the saturation function g_1

FIG. 3. *Fitted functions for empirical probabilities for the Manhattan data set. These figures display results for the conditional frequency estimator used to derive the form of the RPP model. The left figure shows the empirical probability of another event given a previous event a given number of days in the past. The decreasing empirical probability with time motivates our self-excitation function. The right plot shows the increase in propensity for another event given the total cumulative probability from past events. The curvature indicates that additional events have diminishing returns on the likelihood of another event, motivating the saturation component of the RPP.*

the same amount. Instead, we see a distinct curve, indicating that the additional increase in risk decreases as the number of events rises. To further aid in developing a functional form of the model, we fit smooth curves to the data displayed in Figure 3(a) and (b). The process for fitting these smooth curves, as well as simulation experiments for validation, is described in detail in the supplementary material [Ertekin, Rudin and McCormick (2015)]. The fitted values for the smooth curves are

$$g_2(t) = \frac{11.62}{1 + e^{0.039t}},$$

$$g_1(t) = 16.98 \times \left(1 - \log(1 + e^{-0.15t}) \times \frac{1}{\log 2}\right).$$

These estimates inspired the parameterizations we provided in equation (2). We also estimated the baseline hazard rate λ_0 and baseline change C_1 for Manhattan as $\lambda_0 = 2.4225 \times 10^{-4}$ and $C_1 = 0.0512$.

Because the inspection program is relatively new, we were not able to trace out the full functions g_4 and g_3; however, we strongly hypothesize that the inspections have an effect that wears off over time based on a matched pairs study [see, e.g., Passonneau et al. (2011)], where we showed that for manholes that had been inspected at least twice, the second manhole inspection does not lead to the same reduction in vulnerability as the first manhole inspection does. In what follows, we will show how the parameters of g_1, g_2, g_3 and g_4 can be made to specialize to each individual manhole adaptively.

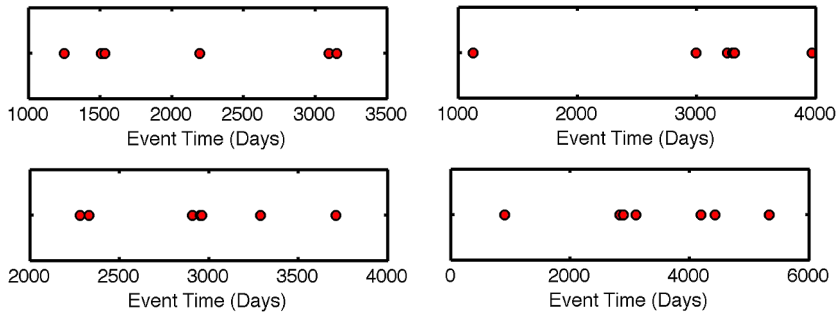

FIG. 4. *Time of events in distinct manholes in the Manhattan data that demonstrate the self-exciting behavior. The x-axis is the number of days elapsed since the day of first record in the data set and the markers indicate the actual time of events.*

Inspired by the CF estimator, we use the family of functions below for fitting power-grid data, where a_1, b_1, a_3, b_3, β and γ are parameters that can be either modeled or fitted:

$$g_1(\omega) = a_1 \times \left(1 - \frac{1}{\log 2}\log\left(1 + e^{-b_1\omega}\right)\right), \qquad g_2(t) = \frac{1}{1 + e^{\beta t}},$$
$$g_3(\omega) = a_3 \times \left(1 - \frac{1}{\log 2}\log\left(1 + e^{b_3\omega}\right)\right), \qquad g_4(t) = \frac{-1}{1 + e^{\gamma t}}. \tag{2}$$

The factors of $\log 2$ ensure that the vulnerability level is not negative.

We need some notation in order to encode the possibility of multiple manholes. In the case that there are multiple entities, there are P time-series, each corresponding to a unique entity p. For medical applications, each p is a patient, and for the electrical grid reliability application, p is a manhole. Our data consist of events $\{t(p)_e\}_{p,e}$, inspections $\{\bar{t}(p)_i\}_{p,i}$ and, additionally, we may have covariate information $M_{p,j}$ about every entity p, with covariates indexed by j. Covariates for the medical application might include a patient's gender, age at the initial time, race, etc. For the manhole events application, covariates include the number of main phase cables in the manhole (number of current carrying cables between two manholes), the total number of cable sets (total number of bundles of cables) including main, service and streetlight cables, and the age of the oldest cable set within the manhole. All covariates were normalized to be between -0.5 and 0.5.

Within the Bayesian framework, we can naturally incorporate the covariates to model functions λ_p for each p adaptively. Consider β in the expression for the self-excitation function g_2 above. The β terms depend on individual-level covariates. In notation,

$$g_2^{(p)}(t) = \frac{1}{1 + e^{\beta(p)t}}, \qquad g_4^{(p)}(t) = \frac{-1}{1 + e^{\gamma(p)t}}. \tag{3}$$

The $\beta^{(p)}$'s are assumed to be generated via a hierarchical model of the form

$$\boldsymbol{\beta} = \log\left(1 + e^{-\mathbf{M}\boldsymbol{\upsilon}}\right) \qquad \text{where } \boldsymbol{\upsilon} \sim N\left(0, \sigma_\upsilon^2\right)$$

are the regression coefficients and $\mathbf{M}$ is the matrix of observed covariates. The $\gamma^{(p)}$'s are modeled hierarchically in the same manner,

$$\boldsymbol{\gamma} = \log(1 + e^{-\mathbf{M}\boldsymbol{\omega}}) \qquad \text{with } \boldsymbol{\omega} \sim N(0, \sigma_\omega^2).$$

This permits slower or faster decay of the self-exciting and self-regulating components based on the characteristics of the individual. For the electrical reliability application, we have noticed that manholes with more cables and older cables tend to have faster decay of the self-exciting terms, for instance.

Demonstrating the need for the saturation function in the RPP model. In the previous section we used exploratory tools on the Manhattan data to demonstrate diminishing returns in risk for multiple subsequent events. In what follows, we link the exploratory work in the last section with our modeling framework, demonstrating how the standard linear self-exciting process can produce unrealistic results under ordinary conditions.

First we show that the self-excitation term can cause the rate of events $\lambda(t)$ to increase without bound. To show this, we considered a baseline vulnerability of $\lambda_0 = 0.01$, setting $C_1 = 0.1$, used $g_2(t) = \frac{1}{1+e^{0.005t}}$, and omitted the other components of the model (no inspections, no saturation g_1). The self-excitation eventually causes the rate of events to escalate unrealistically as shown in Figure 5 (upper left). The embedded subfigure is a zoomed-in version of the first 1500 time steps.

When we include the saturation function g_1, the excitation is controlled, and the probability of an event no longer increases to unreasonable levels. We used $g_1(\omega) = 1 - \frac{1}{\log 2}\log(1 + e^{-\omega})$, so that the vulnerability $\lambda(t)$ can reach to a maximum value of 0.021. The result is in Figure 5 (upper right).

Now we show the effect of the saturation function g_3 in the presence of repeated inspections. If no manhole events occur and the manhole is repeatedly inspected, then using the linear SEPP model, its vulnerability levels can become arbitrarily close to 0. This is not difficult to show, and we do this in Figure 5 (lower left). Here we used $\lambda_0 = 0.2$, $g_4(t) = \frac{-0.25}{1+e^{0.002t}}$, and omitted g_3. We ran the same experiment but with saturation, specifically, with $g_3(\omega) = 1 - \frac{1}{\log 2}\log(1 + e^{\omega})$. The results in Figure 5 (lower right) show that the saturation function never lets the vulnerability drop unrealistically far below the baseline level.

4. Fitting RPP statistical models. In this section we describe our Bayesian framework for inference using RPP models. The RPP intensity in equation (1) provides structure to capture self-excitation, self-regulation and saturation. First, in Section 4.1 we describe the likelihood for the RPP statistical model. We then describe prior distributions and our computational strategy for sampling from the posterior in Section 4.2. Section 4.3 then details the values we use in making predictions. Along with the results presented here, we extensively evaluated our inference strategy using a series of simulation experiments, where the goal is to recover

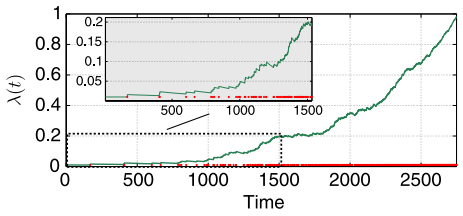

(a) Model with self-excitation function g_2 (without saturation function g_1 and inspections) and a zoomed view of the first 1500 days

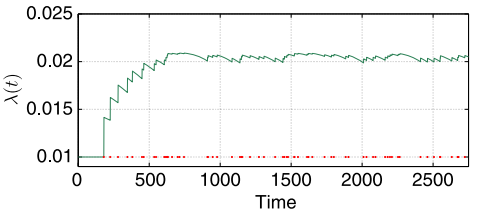

(b) Model with self-excitation function g_2 and saturation function g_1 (no inspections)

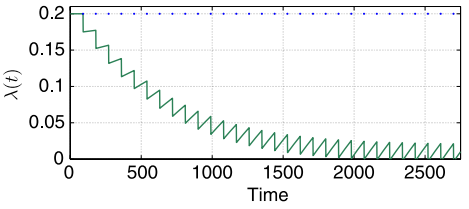

(c) Model with self-regulation function g_4 (without saturation function g_3 and events)

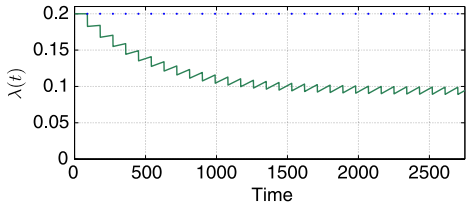

(d) Model with self-regulation function g_4 and saturation function g_3 (no events)

FIG. 5. *The effect of the saturation functions g_1 and g_3. The dots on the time axis in subfigures* (a) *and* (b) *indicate the times of events, and the dots in subfigures* (c) *and* (d) *indicate the times of inspections. The figures on the right include saturation, and the figures on the left do not include saturation. Without saturation, the self-excitation function in* (a) *grows unbounded, whereas the self-regulation function in* (c) *drops to an unrealistic level of zero. The effects of the saturation functions in Figures* (b) *and* (d) *keep g_2 and g_4 within realistic bounds.*

parameters of simulated data for which there is ground truth. We further applied the method of maximum likelihood to the Manhattan power-grid data. Details of these additional experiments are in the supplementary material [Ertekin, Rudin and McCormick (2015)].

4.1. *RPP likelihood.* This section describes the likelihood for the RPP statistical model. Using the intensity function described in Section 3, the RPP likelihood is derived using the likelihood formula for a nonhomogeneous Poisson process over the time interval $[0, T_{\max}]$:

$$\begin{aligned}&\log \mathcal{L}\big(\{t_1^{(p)}, \ldots, t_{N_E^{(p)}}^{(p)}\}_p; \boldsymbol{\upsilon}, a_1, \mathbf{M}\big)\\ &= \sum_{p=1}^{P}\Bigg[\sum_{e=1}^{N_E^{(p)}} \log\big(\lambda_p(t_e^{(p)})\big) - \int_0^{T_{\max}} \lambda_p(u)\,du\Bigg],\end{aligned} \tag{4}$$

where $\boldsymbol{\upsilon}$ are coefficients for covariates represented by the matrix $\mathbf{M}$. The covariates are the number of main phase cables in the manhole (number of current carrying cables between two manholes), the total number of cable sets (total number of

bundles of cables) including main, service and streetlight cables, and the age of the oldest cable set within the manhole. All covariates were normalized to be between -0.5 and 0.5.

4.2. *Bayesian RPP.* Developing a Bayesian framework facilitates sharing of information between observably similar manholes, thus making more efficient use of available covariate information. The RPP model encodes much of our prior information into the shape of the rate function given in equation (1). As discussed in Section 3, we opted for a simple, parsimonious model that imposes mild regularization and information sharing without adding substantial additional information; specifically, we use diffuse Gaussian priors on the log scale for each regression coefficient.

We fit the model using Approximate Bayesian Computation [Diggle and Gratton (1984)]. The principle of Approximate Bayesian Computation (ABC) is to randomly choose proposed parameter values, use those values to generate data, and then compare the generated data to the observed data. If the difference is sufficiently small, then we accept the proposed parameters as draws from the approximate posterior. To do ABC, we need two things: (i) to be able to simulate from the model and (ii) a summary statistic. To compare the generated and observed data, the summary statistic from the observed data, $S(\{t_1^{(p)}, \ldots, t_{N_E^{(p)}}^{(p)}\}_p)$, is compared to that of the data simulated from the proposed parameter values, $S(\{t_1^{(p),\mathrm{sim}}, \ldots, t_{N_E^{(p),\mathrm{sim}}}^{(p),\mathrm{sim}}\}_p)$. If the values are similar, it indicates that the proposed parameter values may yield a useful model for the data.

A critical difference between updating a parameter value in an ABC iteration versus, for example, a Metropolis–Hastings step is that ABC requires simulating from the likelihood, whereas Metropolis–Hastings requires evaluating the likelihood. In our context, we are able to both evaluate and simulate from the likelihood with approximately the same computational complexity. ABC has some advantages, namely, that we have meaningful summary statistics, discussed below. Further, in our case it is not particularly computationally challenging, as we already extensively simulate from the model as a means of evaluating hypothetical inspection policies. We evaluated the adequacy of this method extensively in simulation studies presented in the supplementary material [Ertekin, Rudin and McCormick (2015)].

A key conceptual aspect of ABC is that one can choose the summary statistic to best match the problem. The sufficient statistic for the RPP is the vector of event times, and thus gives no data reduction—so we choose other statistics. One important insight in constructing our summary statistic is that changing the parameters in the RPP model alters the distribution of times between events. The histogram of time differences for a homogenous Poisson Process, for example, has an exponential decay. The self-exciting process, on the other hand, has a distribution resembling a lognormal because of the positive association between intensities after an

event occurs. Altering the parameters of the RPP model changes the intensity of self-excitation and self-regulation, thus altering the distribution of times between events. We construct our first statistic, therefore, by examining the KL divergence between the distribution of times between events in the data and the distribution between event times in the simulated data. We do this for each of our proposed parameters. Examining the distribution of times between events, though not the true sufficient statistic, captures a concise and low-dimensional summary of a key feature of the process. This statistic does not, however, capture the overall prevalence of events in the process. Since we focus only on the *distribution* of times between events, various processes with different overall intensity could produce distributions with similar KL divergence to the data distribution. We therefore introduce a second statistic that counts the total number of events. We contend that together these statistics represent both the spacing and the overall scale (or frequency) of events. Thus, the two summary measures we use are as follows:

1. DNE: The difference in the number of events in the simulated and observed data.
2. KL: The Kullback–Leibler divergence between two histograms, one from the observed data and one from the real data. These are histograms of time differences between events.

For the NYC data, we visualized three-dimensional parameter values, both for DNE (in Figure 6) and KL (in Figure 7) metrics. In both figures, smaller values (dark blue) are better. As seen, the regions where KL and DNE are optimized are very similar.

Denoting the probability distribution of the actual data as P and the probability distribution of the simulated data as Q_v, KL Divergence is computed as

$$\mathrm{KL}(P \| Q_v) = \sum_{\text{bin}} \ln\left(\frac{P(\text{bin})}{Q_v(\text{bin})}\right) P(\text{bin}).$$

As mentioned previously in this section, the Bayesian portion of our model is relatively parsimonious but does impose mild regularization and encourages sta-

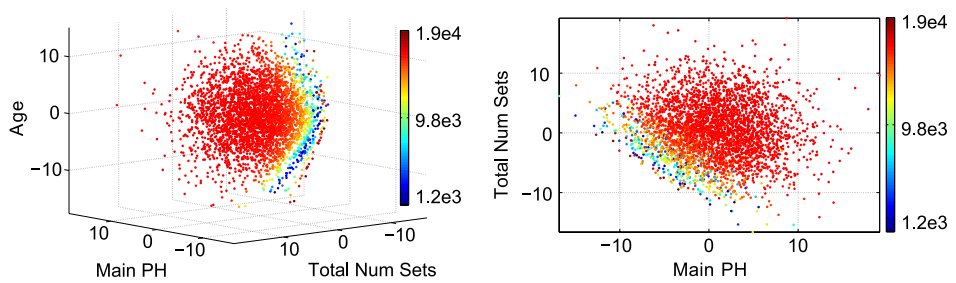

FIG. 6. *DNE for Manhattan data set. Each axis corresponds to the coefficient for one of the covariates. The magnitude of DNE is indicated by the color.*

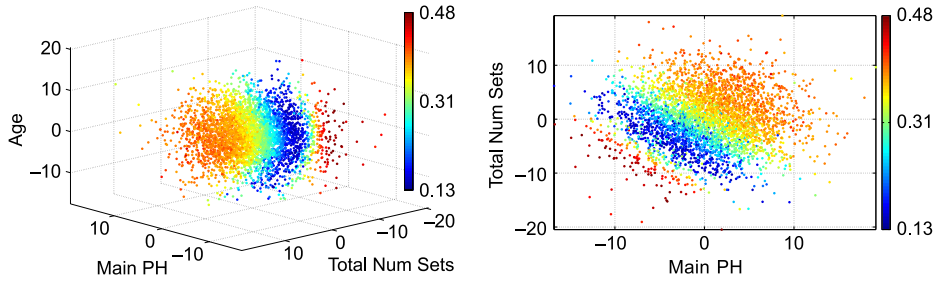

FIG. 7. *KL for Manhattan data set. Each axis corresponds to the coefficient for one of the covariates. The magnitude of KL is indicated by the color.*

bility. We require a distribution π over parameter values. If covariates are not used, π is a distribution over β (and γ if inspections are present). If covariates are used, π is a distribution over $\boldsymbol{\upsilon}$ and $\boldsymbol{\omega}$. One option for π is a uniform distribution across a grid of reasonable values. Another option, which was used in our experiments, is to simulate from diffuse Gaussian/weakly informative priors on the log scale [e.g., draw $\log(\upsilon_j) \sim N(0, 5)$]. We assumed that C_1 and a_1 can be treated as tuning constants to be estimated using the CF estimator method, though it is possible to define priors on these quantities as well if desired.

There is an increasingly large literature in both the theory and implementation of ABC [see, e.g., Beaumont et al. (2009), Drovandi, Pettitt and Faddy (2011), Fearnhead and Prangle (2012)] that could be used to produce estimates of the full posterior. In the supplementary material [Ertekin, Rudin and McCormick (2015)], we present an importance sampling algorithm as one possible approach. In our work, however, the goal is to estimate the posterior mode, which we then use for prediction. To verify our ABC procedure, we used simulated ground truth data with known β and γ values, and attempted to recover these values with the ABC method, for both the DNE and KL metrics. We performed extensive simulation studies to evaluate this method and full results are given in the supplementary material [Ertekin, Rudin and McCormick (2015)].

In the next section we discuss how we estimate the posterior mode by using a manifold approximation to the region of high posterior density. We begin by generating a set of proposed parameter values using the prior distributions. Consistent with ABC, we simulate data from each set of candidate values and compare the simulated data to our observed data using the KL and DNE statistics described above. (From here, we could, e.g., define a kernel and accept draws with a given probability as in importance sampling. Instead, our goal is estimating the posterior mode to find parameters for the policy decision, as we describe next.)

4.3. *Choosing parameter values for the policy decision.* For the policy simulation in Section 6 we wish to choose one set of parameter values to inform our

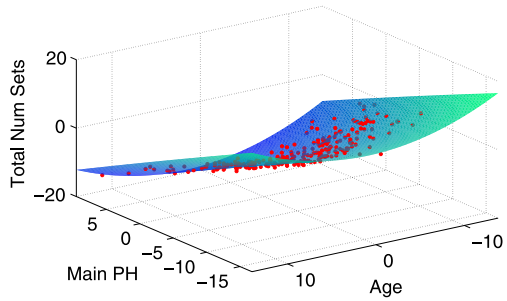

FIG. 8. *Fitted manifold of $\boldsymbol{\upsilon}$ values with smallest KL divergence and smallest DNE.*

decision. In order to choose a single best value of the parameters, we fit a polynomial manifold to the intersection of the bottom 10% of KL values and the bottom 10% of DNE values. Defining υ_1, υ_2 and υ_3 as the coefficients for number of main phase cables, age of oldest main cable set and total number of sets features, the formula for the manifold is

$$\upsilon_3 = -9.6 - 0.98\upsilon_1 - 0.13\upsilon_2 - 1.1 \times 10^{-3}(\upsilon_1)^2 - 3.6 \times 10^{-3}\upsilon_1\upsilon_2 + 4.67 \times 10^{-2}(\upsilon_2)^2,$$

which is determined by a least squares fit to the data. The fitted manifold is shown in Figure 8 along with the data.

We then optimized for the point on the manifold closest to the origin. This implicitly adds regularization, as it chooses the parameter values closest to the origin. This point is $\upsilon_1 = -4.6554$, $\upsilon_2 = -0.5716$, and $\upsilon_3 = -4.8028$.

Note that cable age (corresponding to the second coefficient) is not the most important feature defining the manifold. As previous studies have shown [Rudin et al. (2010)], even though there are very old cables in the city, the age of cables within a manhole is not alone the best predictor of vulnerability. Now we also know that it is not the best predictor of the rate of decay of vulnerability back to baseline levels. This supports Con Edison's goal to prioritize the most vulnerable components of the power-grid, rather than simply replacing the oldest components. The features that mainly determine decay of the self-excitation function g_2 are the number of main phase cables and the number of cable sets. As either or both of these numbers increase, decay rate β increases, meaning that manholes with more cables tend to return to baseline levels faster than manholes with fewer cables.

5. Predicting events on the NYC power-grid. Our first experiment aims to evaluate whether the CF estimator or the feature-based strategy introduced above is better in terms of identifying the most vulnerable manholes. To do this, we selected 5000 manholes (rank 1001–6000 from the project's current long-term prediction model). These manholes have similar vulnerability levels, which allows us to isolate the self-exciting effect without modeling the baseline level. Using both

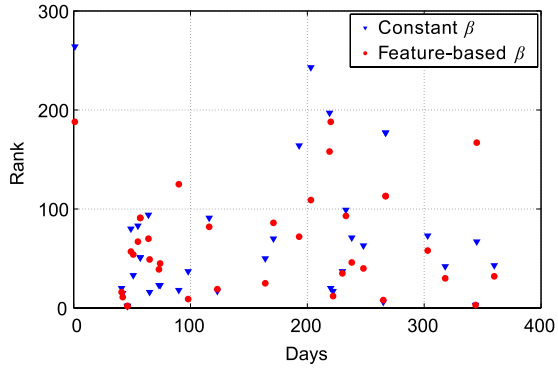

FIG. 9. *Ranking differences between feature-based and constant (nonfeature-based) β strategies.*

the feature-based β (ABC, with KL metric) and constant β (CF estimator method) strategies, the models were trained on data through 2009, and then we estimated the vulnerabilities of the manholes on December 31st, 2009. These vulnerabilities were used as the *initial* vulnerabilities for an evaluation on the 2010 event data. 2010 is a relevant year because the first inspection cycle ended in 2009. All manholes had been inspected at least once, and many were inspected toward the end of 2009, which stabilizes the inspection effects. For each of the 53K manholes and at each of the 365 days of 2010, when we observed a serious event in a manhole p, we evaluated the rank of that manhole with respect to both the feature-based and nonfeature-based models, where rank represents the number of manholes that were given higher vulnerabilities than manhole p. As our goal is to compare the relative rankings provided by the two strategies, we consider only events where the vulnerabilities assigned by both strategies are different than the baseline vulnerability. Figure 9 displays the ranks of the manholes on the day of their serious event. A smaller rank indicates being higher up the list, thus lower is better. Overall, we find that the feature-based β strategy performs better than the nonfeature-based strategy over all of the rank comparisons in 2010 (p-value 0.09, sign test). Our results mainly illustrate that using different decay rates on past events for different types of manholes leads to better predictions. Recall from Section 4.3 that larger manholes tend to recover faster from previous events. The approach without the features ignores the differences between manholes, and uses the same decay rate, whereas the feature-based RPP takes these decay rates into account in making predictions.

In the second experiment, we compared the feature-based β strategy to the Cox proportional–hazard model, which is commonly used in survival analysis to assess the probability of failure in mechanical systems. We employed this model to assess the likelihood of a manhole having a serious event on a particular day. For each manhole, we used the same three static covariates as in the feature-based β model, and developed four time-dependent features. The time-varying features for

day t are (1) the number of times the manhole was a trouble hole (source of the problem) for a serious event until t, (2) the number of times the manhole was a trouble hole for a serious event in the last year, (3) the number of times the manhole was a trouble hole for a precursor event (less serious event) until t, and (4) the number of times the manhole was a trouble hole for a precursor event in the last year. The feature-based β model currently does not differentiate serious and precursor events, though it is a direct extension to do this if desired. The model was trained using the coxph function in the R survival package using data prior to 2009, and then predictions were made on the test set of 5000 manholes in the 2010 data set. These predictions were transformed into ranked lists of manholes for each day. We then compared the ranks achieved by the Cox model with the ranks of manholes at the time of events. The difference of aggregate ranks was in favor of the feature-based β approach (p-value 7e–06, sign test), indicating that the feature-based β strategy provides a substantial advantage in its ability to prioritize vulnerable manholes.

The Cox model we compared with represents a "long-term" model similar to what we were using previously for manhole event prediction on Con Edison data [Rudin et al. (2010)]. The Cox model considers different information, namely, counts of past events. These counts are time-varying, but the past events do not smoothly wear off in time as they do for the RPP. The fact that the RPP model is competitive with the Cox model indicates that the effects of past manhole events do wear off with time (in agreement with Figure 3 where we traced the decay directly using data). The saturating elements of the model ensure that the model is physically plausible, since we showed in Section 3 that the results could be unphysical (with rates going to 0 or above 1) without the saturation.

6. Making broader policy decisions using RPPs. Because the RPP model is a generative model, it can be used to simulate the future, and thus assist with broader policy decisions regarding how often inspections should be performed. This can be used to justify allocation of spending. Con Edison's existing inspection policy is a combination of targeted periodic inspections and ad hoc inspections. The targeted inspections are planned in advance, whereas the ad hoc inspections are unscheduled. An ad hoc inspection could be performed while a utility worker is in the process of, for instance, installing a new service cable to a building or repairing an outage. Either source of inspection can result in an urgent repair (Type I), an important but not urgent repair (Type II), a suggested structural repair (Types III and IV), or no repair, or any combination of repairs. Urgent repairs need to be completed before the inspector leaves the manhole, whereas Type IV repairs are placed on a waiting list. According to the current inspections policy, each manhole undergoes a targeted inspection every 5 years. The choice of inspection policy to simulate can be determined very flexibly, and any inspection policy and hypothesized effect of inspections can be examined through simulation.

As a demonstration, we conducted a simulation over a 20 year future time horizon that permits a cost-benefit analysis of the inspection program, when targeted inspections are performed at a given frequency. To do this simulation, we require the following:

- A characterization of manhole vulnerability. For Manhattan, this is learned from the past using the ABC RPP feature-based β training strategy for the saturation function g_1 and the self-excitation function g_2 discussed above. Saturation and self-regulation functions g_3 and g_4 for the inspection program cannot yet be learned due to the newness of the inspection program and are discussed below.
- An inspection policy. The policy can include targeted, ad hoc or history-based inspections. We chose to evaluate "bright line" inspection policies, where each manhole is inspected once in each Y year period, where Y is varied (discussed below). We also included an ad hoc inspection policy that visits 3 manholes per day on average.

Effect of inspections: The effect of inspections on the overall vulnerability of manholes were designed in consultation with domain experts. The choices are somewhat conservative, so as to give a lower bound for costs. The effect of an urgent repair (Type I) is different from the effect of less urgent repairs (Types II, III and IV). For all inspection types, after 1 year beyond the time of the inspection, the effect of the inspection decays to, on average, 85% of its initial effect, in agreement with a short-term empirical study on inspections. (There is some uncertainty in this initial effect, and the initial drop in vulnerability is chosen from a normal distribution so that after one year the effect decays to a mean of 85%.) For Type I inspections, the effect of the inspection decays to baseline levels after approximately 3000 days, and for Types II, III and IV, which are more extensive repairs, the effect fully decays after 7000 days. In particular, we use the following g_4 functions:

$$g_4^{\text{Type I}}(t) = -83.7989 \times \left(r \times 5 \times 10^{-4} + 3.5 \times 10^{-3}\right) \times \frac{1}{1 + e^{0.0018t}}, \tag{5}$$

$$g_4^{\text{Types II,III,IV}}(t) = -49.014 \times \left(r \times 5 \times 10^{-4} + 7 \times 10^{-3}\right) \times \frac{1}{1 + e^{0.00068t}}, \tag{6}$$

where r is randomly sampled from a standard normal distribution. For all inspection types, we used the following g_3 saturation function:

$$g_3(t) = 0.4 \times \left(1 - \log\left(1 + e^{-3.75t}\right) \times \frac{1}{\log 2}\right),$$

which ensures that subsequent inspections do not lower the vulnerability to more than 60% of the baseline vulnerability. Sampled g_4 functions for Type I and Types II, II, IV, along with g_3 are shown in Figure 10.

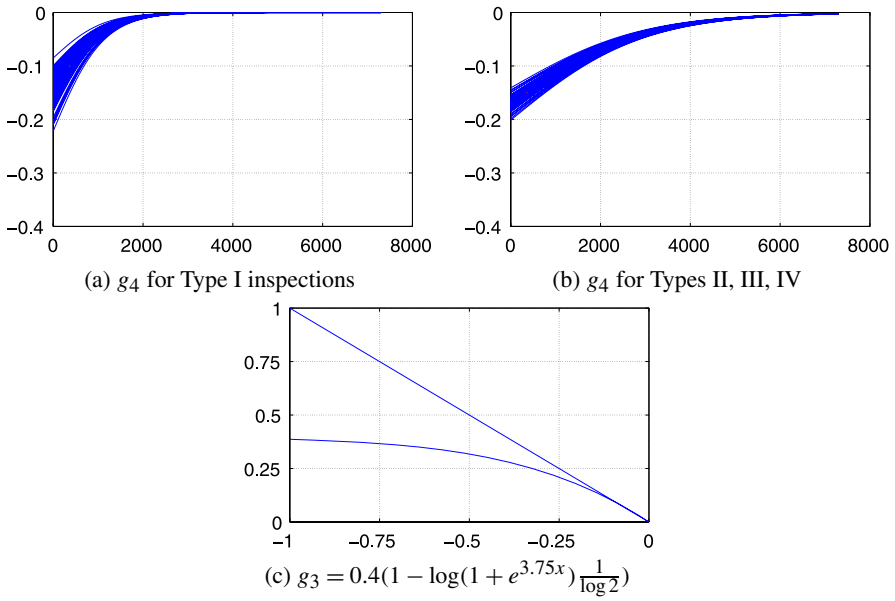

(a) g_4 for Type I inspections

(b) g_4 for Types II, III, IV

(c) $g_3 = 0.4(1 - \log(1 + e^{3.75x})\frac{1}{\log 2})$

FIG. 10. *Saturation and self-regulation functions g_3 and g_4 for simulation.*

One targeted inspection per manhole was distributed randomly across Y years for the bright line Y-year inspection policies, and $3 \times 365 = 1095$ ad hoc inspections for each year were uniformly distributed, which corresponds to 3 ad hoc inspections per day for the whole power grid on average. During the simulation, when we arrived at a time step with an inspection, the inspection outcome was Type I with 25% probability, or one of Types II, III or IV, with 25% probability. In the rest of the cases (50% probability), the inspection was clean, and the manhole's vulnerability was not affected by the inspection. If the inspection resulted in a repair, we sampled r randomly and randomly chose the inspection outcome (Type I or Types II, III, IV). This percentage breakdown was observed approximately for a recent year of inspections in NYC.

To initialize manhole vulnerabilities for a bright line policy of Y years, we simulated the previous Y-year inspection cycle and started the simulation with the vulnerabilities obtained at the end of this full cycle.

Simulation results: We simulated events and inspections for 53.5K manholes for bright line policies ranging from $Y = 1$ year to $Y = 20$ years. Naturally, a longer inspection cycle corresponds to fewer daily inspections, which translates into an increase in overall vulnerabilities and an increase in the number of events. This is quantified in Figure 11, which shows the projected number of inspections and events for each Y year bright line policy. If we change from a 6 year bright line inspection policy to a 4 year policy, we estimate a reduction of approximately 100 events per year. The relative costs of inspections and events can thus be considered in order to justify a particular choice of Y for the bright line policy.

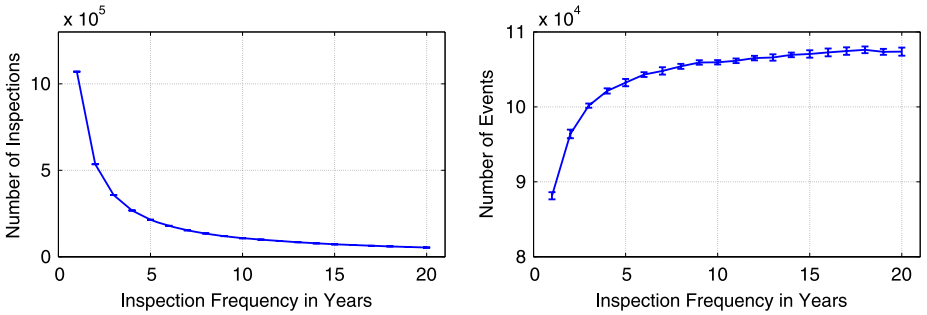

FIG. 11. *Number of events and inspections based on bright line policy. Number of years Y for the bright line policy is on the horizontal axis in both figures. The left figure shows the number of inspections, the right figure shows the number of events.*

Let us say, for instance, that each inspection costs C_I and each event costs C_E. The simulation results allow us to denote the forecasted expected number of events over a period of time T as a function of the inspection frequency Y, which we denote by $N_E(Y, T)$. The value of $N_E(Y, T)$ comes directly from the simulation, as plotted in Figure 11. Let us make a decision for Y for P total manholes, over a period T. To do this, we would choose a Y that minimizes the total cost

$$C_E \times N_E(Y, T) + C_I \times P \times T/Y.$$

This line of reasoning provides a quantitative mechanism for decision making and can be used to justify a particular choice of inspection policy.

7. Conclusion. Keeping our electrical infrastructure safe and reliable is of critical concern, as power outages affect almost all aspects of our society, including hospitals, financial centers, data centers, transportation and supermarkets. If we are able to combine historical data with the best available statistical tools, it will be possible to impact our ability to maintain an ever aging and growing power grid. In this work, we presented a methodology for modeling power-grid failures that is based on natural assumptions: (i) that power failures have a self-exciting property, which was hypothesized by Con Edison engineers, (ii) that the power company's actions are able to regulate vulnerability levels, (iii) that the effects on the vulnerability level of past events or repairs can saturate, and (iv) that vulnerability estimates should be similar between similar entities. We have been able to show directly (using the CF estimator for the RPP) that the self-exciting and saturation assumptions hold. We demonstrated through experiments on past power-grid data from NYC, and through simulations, that the RPP model is able to capture the relevant dynamics well enough to predict power failures better than the current approaches in use.

The modeling assumptions that underlie RPPs can be directly ported to other problems. RPPs are a natural fit for problems in healthcare, where medical

conditions cause self-excitation and treatments provide regulation. Through the Bayesian framework we introduced, RPPs extend to a broad range of problems where predictive power can be pooled among multiple related entities, whether manholes or medical patients.

The results presented in this work show for the first time that manhole events can be predicted in the short term, which was previously thought not to be possible. Knowing how one might do this permits us to take preventive action to keep vulnerability levels low, and can help make broader policy decisions for power-grid maintenance through simulation of many uncertain futures, simulated over any desired policy.

SUPPLEMENTARY MATERIAL

Supplementary material for "Reactive point processes: A new approach to predicting power failures in underground electrical systems" (DOI: 10.1214/14-AOAS789SUPP; .pdf). The supplementary material includes an expanded related work section, conditional frequency estimator (CF estimator) for the RPP, experiments with a maximum likelihood approach, a description of the inspection policy used in Section 6, an analysis of Manhattan data using random effects model and simulation studies for validating the fitting techniques for the models in the paper. It also includes a description and link for a publicly available simulated data set that we generated, based on statistical properties of the Manhattan data set.

REFERENCES

AÏT-SAHALIA, Y., CACHO-DIAZ, J. and LAEVEN, R. J. (2010). Modeling financial contagion using mutually exciting jump processes. Technical report, National Bureau of Economic Research, Cambridge, MA.

BACRY, E., DELATTRE, S., HOFFMANN, M. and MUZY, J. F. (2013). Modelling microstructure noise with mutually exciting point processes. *Quant. Finance* **13** 65–77. MR3005350

BARTLETT, M. S. (1963). The spectral analysis of point processes. *J. R. Stat. Soc. Ser. B Stat. Methodol.* **25** 264–296. MR0171334

BEAUMONT, M. A., CORNUET, J.-M., MARIN, J.-M. and ROBERT, C. P. (2009). Adaptive approximate Bayesian computation. *Biometrika* **96** 983–990. MR2767283

BLUNDELL, C., BECK, J. and HELLER, K. A. (2012). Modelling reciprocating relationships with Hawkes processes. In *Advances in Neural Information Processing Systems* 25. Curran Associates, Red Hook, NY.

CHEHRAZI, N. and WEBER, T. A. (2011). Dynamic valuation of delinquent credit-card accounts. Working paper.

CRANE, R. and SORNETTE, D. (2008). Robust dynamic classes revealed by measuring the response function of a social system. *Proc. Natl. Acad. Sci. USA* **105** 15649–15653.

DIGGLE, P. J. and GRATTON, R. J. (1984). Monte Carlo methods of inference for implicit statistical models. *J. R. Stat. Soc. Ser. B Stat. Methodol.* **46** 193–227. MR0781880

DOE (2008). The Smart Grid, An Introduction. Technical report. Prepared by Litos Strategic Communication. US Dept. Energy, Office of Electricity Delivery & Energy Reliability.

DROVANDI, C. C., PETTITT, A. N. and FADDY, M. J. (2011). Approximate Bayesian computation using indirect inference. *J. R. Stat. Soc. Ser. C. Appl. Stat.* **60** 317–337. MR2767849

DU, N., SONG, L., WOO, H. and ZHA, H. (2013). Uncover topic-sensitive information diffusion networks. In *Proceedings of the Sixteenth International Conference on Artificial Intelligence and Statistics* 229–237.

EGESDAL, M., FATHAUER, C., LOUIE, K., NEUMAN, J., MOHLER, G. and LEWIS, E. (2010). Statistical and stochastic modeling of gang rivalries in Los Angeles. *SIAM Undergraduate Research Online* **3** 72–94.

EMBRECHTS, P., LINIGER, T. and LIN, L. (2011). Multivariate Hawkes processes: An application to financial data. *J. Appl. Probab.* **48A** 367–378. MR2865638

ERTEKIN, S., RUDIN, C. and MCCORMICK, T. (2013). Predicting Power Failures with Reactive Point Processes. In *AAAI Workshop on Late-Breaking Developments*. AAAI Press, Menlo Park, CA.

ERTEKIN, S., RUDIN, C. and MCCORMICK, T. H. (2015). Supplement to "Reactive point processes: A new approach to predicting power failures in underground electrical systems." DOI:10.1214/14-AOAS789SUPP.

FEARNHEAD, P. and PRANGLE, D. (2012). Constructing summary statistics for approximate Bayesian computation: Semi-automatic approximate Bayesian computation. *J. R. Stat. Soc. Ser. B Stat. Methodol.* **74** 419–474. MR2925370

FILIMONOV, V. and SORNETTE, D. (2012). Quantifying reflexivity in financial markets: Toward a prediction of flash crashes. *Phys. Rev. E* (3) **85** 056108.

GUTTORP, P. and THORARINSDOTTIR, T. L. (2012). Bayesian inference for non-Markovian point processes. In *Advances and Challenges in Space–Time Modeling of Natural Events* (E. Porcu, J.-M. Montero and M. Schlather, eds.) 79–102. Springer, Berlin.

HARDIMAN, S. J., BERCOT, N. and BOUCHAUD, J.-P. (2013). Critical reflexivity in financial markets: A Hawkes process analysis. *Eur. Phys. J. B* **86** 1–9.

JOHNSON, D. H. (1996). Point process models of single-neuron discharges. *J. Comput. Neurosci.* **3** 275–299.

KERSTAN, J. (1964). Teilprozesse Poissonscher Prozesse. In *Trans. Third Prague Conf. Information Theory, Statist. Decision Functions, Random Processes* (*Liblice*, 1962) 377–403. Publ. House Czech. Acad. Sci., Prague. MR0166826

KRUMIN, M., REUTSKY, I. and SHOHAM, S. (2010). Correlation-based analysis and generation of multiple spike trains using hawkes models with an exogenous input. *Front. Comput. Neurosci.* **4** 147.

LEWIS, E., MOHLER, G., BRANTINGHAM, P. J. and BERTOZZI, A. (2010). Self-exciting point process models of insurgency in Iraq. UCLA CAM Reports 10-38.

LOUIE, K., MASAKI, M. and ALLENBY, M. (2010). A point process model for simulating gang-on-gang violence. Technical report, UCLA.

MASUDA, N., TAKAGUCHI, T., SATO, N. and YANO, K. (2012). Self-exciting point process modeling of conversation event sequences. Preprint. Available at arXiv:1205.5109.

MITCHELL, L. and CATES, M. E. (2010). Hawkes process as a model of social interactions: A view on video dynamics. *J. Phys. A* **43** 045101, 11. MR2578723

MOHLER, G. O., SHORT, M. B., BRANTINGHAM, P. J., SCHOENBERG, F. P. and TITA, G. E. (2011). Self-exciting point process modeling of crime. *J. Amer. Statist. Assoc.* **106** 100–108. MR2816705

NYBC (2010). Electricity OUTLOOK: Powering New York City's economic future. Technical report. New York Building Congress Reports: Energy Outlook 2010–2025.

OGATA, Y. (1988). Statistical models for earthquake occurrences and residual analysis for point processes. *J. Amer. Statist. Assoc.* **83** 9–27.

OGATA, Y. (1998). Space–time point-process models for earthquake occurrences. *Ann. Inst. Statist. Math.* **50** 379–402.

PASSONNEAU, R., RUDIN, C., RADEVA, A., TOMAR, A. and XIE, B. (2011). Treatment effect of repairs to an electrical grid: Leveraging a machine learned model of structure vulnerability. In *Proceedings of the KDD Workshop on Data Mining Applications in Sustainability* (*SustKDD*), 17*th Annual ACM SIGKDD Conference on Knowledge Discovery and Data Mining*. ACM, New York.

PERUGGIA, M. and SANTNER, T. (1996). Bayesian analysis of time evolution of earthquakes. *J. Amer. Statist. Assoc.* **91** 1209–1218.

PORTER, M. D. and WHITE, G. (2012). Self-exciting hurdle models for terrorist activity. *Ann. Appl. Stat.* **6** 106–124. MR2951531

REYNAUD-BOURET, P. and SCHBATH, S. (2010). Adaptive estimation for Hawkes processes; application to genome analysis. *Ann. Statist.* **38** 2781–2822. MR2722456

RHODES, L. (2013). US power grid has issues with reliability. Data Center Knowledge (www.datacenterknowledge.com): Industry Perspectives.

RUDIN, C., PASSONNEAU, R. J., RADEVA, A., DUTTA, H., IEROME, S. and ISAAC, D. (2010). A process for predicting manhole events in Manhattan. *Mach. Learn.* **80** 1–31. MR3108158

RUDIN, C., WALTZ, D., ANDERSON, R. N., BOULANGER, A., SALLEB-AOUISSI, A., CHOW, M., DUTTA, H., GROSS, P. N., HUANG, B., IEROME, S., ISAAC, D. F., KRESSNER, A., PASSONNEAU, R. J., RADEVA, A. and WU, L. (2012). Machine learning for the New York City power grid. *IEEE Trans. Pattern. Anal. Mach. Intell.* **34** 328–345.

RUDIN, C., ERTEKIN, S., PASSONNEAU, R., RADEVA, A., TOMAR, A., XIE, B., LEWIS, S., RIDDLE, M., PANGSRIVINIJ, D. and MCCORMICK, T. (2014). Analytics for power grid distribution reliability in New York City. *Interfaces* **44** 364–383.

SIMMA, A. and JORDAN, M. I. (2010). Modeling Events with Cascades of Poisson Processes. In *Proc. of the* 26*th Conference on Uncertainty in Artificial Intelligence* (*UAI*2010). *AUAI Press*.

SO, H. (2004). Council approves bill on Con Ed annual inspections. *The Villager* **74** 23.

TADDY, M. A. and KOTTAS, A. (2012). Mixture modeling for marked Poisson processes. *Bayesian Anal.* **7** 335–361. MR2934954

Ş. ERTEKIN
C. RUDIN
MIT COMPUTER SCIENCE
AND ARTIFICIAL INTELLIGENCE LABORATORY
AND
MIT SLOAN SCHOOL OF MANAGEMENT
MASSACHUSETTS INSTITUTE OF TECHNOLOGY
CAMBRIDGE, MASSACHUSETTS 02139
USA
E-MAIL: seyda@mit.edu
rudin@mit.edu

T. H. MCCORMICK
DEPARTMENT OF STATISTICS
UNIVERSITY OF WASHINGTON
SEATTLE, WASHINGTON 98195
USA
E-MAIL: tylermc@u.washington.edu